Proximal nerve magnetization transfer MRI relates to disability in Charcot-Marie-Tooth diseases

Richard D. Dortch, PhD
Lindsey M. Dethrage, MS
John C. Gore, PhD
Seth A. Smith, PhD
Jun Li, MD, PhD

Correspondence to
Dr. Dortch:
richard.dortch@vanderbilt.edu

ABSTRACT

Objective: The objectives of this study were (1) to develop a novel magnetization transfer ratio (MTR) MRI assay of the proximal sciatic nerve (SN), which is inaccessible via current tools for assessing peripheral nerves, and (2) to evaluate the resulting MTR values as a potential biomarker of myelin content changes in patients with Charcot-Marie-Tooth (CMT) diseases.

Methods: MTR was measured in the SN of patients with CMT type 1A (CMT1A, n = 10), CMT type 2A (CMT2A, n = 3), hereditary neuropathy with liability to pressure palsies (n = 3), and healthy controls (n = 21). Additional patients without a genetically confirmed subtype (n = 4), but whose family histories and electrophysiologic tests were consistent with CMT, were also included. The relationship between MTR and clinical neuropathy scores was assessed, and the interscan and inter-rater reliability of MTR was estimated.

Results: Mean volumetric MTR values were significantly decreased in the SN of patients with CMT1A (33.8 ± 3.3 percent units) and CMT2A (31.5 ± 1.9 percent units) relative to controls (37.2 ± 2.3 percent units). A significant relationship between MTR and disability scores was also detected ($p = 0.01$ for genetically confirmed patients only, $p = 0.04$ for all patients). From interscan and inter-rater reliability analyses, proximal nerve MTR values were repeatable at the slicewise and mean volumetric levels.

Conclusions: MTR measurements may be a viable biomarker of proximal nerve pathology in patients with CMT. *Neurology*® 2014;83:1545–1553

GLOSSARY

BMI = body mass index; **CMAP** = compound motor action potential; **CMT** = Charcot-Marie-Tooth; **CMT1** = Charcot-Marie-Tooth type 1; **CMT2** = Charcot-Marie-Tooth type 2; **CMTNS** = Charcot-Marie-Tooth neuropathy score; **$CMTNS_C$** = clinical Charcot-Marie-Tooth neuropathy score; **$CMTNS_L$** = leg-specific Charcot-Marie-Tooth neuropathy score; **CSA_{SN}** = cross-sectional area of the sciatic nerve; **HNPP** = hereditary neuropathy with liability to pressure palsies; **ICC** = intraclass correlation coefficient; **MCV** = motor conduction velocity; **MT** = magnetization transfer; **MTR** = magnetization transfer ratio; **MTR_s** = magnetization transfer ratio values calculated for each slice; **MTR_v** = magnetization transfer ratio values calculated across the entire volume; **NCS** = nerve conduction studies; ***PMP22*** = peripheral myelin protein 22 gene; **pu** = percent units; **RC** = repeatability coefficient; **ROI** = region of interest; **SN** = sciatic nerve.

Charcot-Marie-Tooth (CMT) diseases are a group of inherited neuropathies that affect motor and sensory nerves. A majority of CMT phenotypes can be classified as primary demyelination/dysmyelinating (CMT1) or primary axonal (CMT2) neuropathies.[1,2] CMT type 1A (CMT1A ≈ 80% of CMT1 cases[3,4]) arises from duplication of the peripheral myelin protein 22 (*PMP22*) gene[5,6] and results in dysmyelination and secondary axonal loss.[7] CMT type 2A (CMT2A ≈ 35% of CMT2 cases[8]) is caused by missense mutations in the gene that encodes for mitofusin 2[9] and leads to primary axonal degeneration.[8] Although the pathologic features of CMT1A/CMT2A are different, length-dependent axonal loss occurs in both and is predictive of outcomes.[10]

Current tools for assessing patients with CMT include nerve conduction studies (NCS), skin biopsies,[11] and CMT neuropathy scores (CMTNS).[10] These techniques are typically limited to the study of distal nerves, which are often severely damaged and, therefore, unavailable for these

From the Department of Radiology and Radiological Sciences (R.D.D., J.C.G., S.A.S.), Vanderbilt University Institute of Imaging Science (R.D.D., L.M.D., J.C.G., S.A.S.), and the Departments of Biomedical Engineering (R.D.D., J.C.G., S.A.S.), Physics and Astronomy (J.C.G., S.A.S.), Molecular Physiology and Biophysics (J.C.G.), and Neurology (J.L.), Vanderbilt University, Nashville, TN.

Go to Neurology.org for full disclosures. Funding information and disclosures deemed relevant by the authors, if any, are provided at the end of the article.

tests. Due in part to this limitation, recent CMT1A clinical trials[12,13] noted difficulty in detecting disease progression when using CMTNS as an outcome measure. In addition, quality of life assessments have shown little sensitivity to disease progression.[14]

Proximal nerves are partially preserved in patients with CMT, and may be an ideal target for tracking disease progression and treatment response. Although these nerves are inaccessible via current tools, certain MRI techniques may be suited for probing proximal nerves. For example, MRI of muscle[15–17] is sensitive to the downstream effects of nerve denervation on muscle. Nerve pathology can also be probed directly via quantitative MRI techniques. For example, diffusion MRI of peripheral nerves yields metrics that relate to disability[18,19]; however, this method often requires longer, lower resolution acquisitions than desired. Similar to diffusion MRI, magnetization transfer ratio (MTR) imaging is sensitive to changes in myelin density that can occur from demyelination or axonal loss,[20] and fast, high-resolution MTR imaging of peripheral nerves is feasible.[21] Therefore, we have developed and tested a novel MTR assay of the sciatic nerve (SN) as a potential biomarker in patients with CMT.

METHODS

Human subjects and clinical information. MRI was performed on 21 healthy volunteers with no known history of peripheral neuropathy (control subjects) and 16 patients with a genetically confirmed inherited neuropathy (10 CMT1A, 3 CMT2A, and 3 hereditary neuropathy with liability to pressure palsies [HNPP]). Data were also collected from 4 patients with CMT with unknown genetic causes, but who were diagnosed based on family/clinical history and NCS. Patients were recruited from the Vanderbilt University CMT Clinic, which is part of the international CMT Consortium. No patient had a history of diabetes, renal failure, HIV infection, or other conditions linked to peripheral neuropathies. The span of ages and body mass indices (BMIs) in the control subjects approximately matched the span of values in patients with CMT (table). A subset of participants was evaluated using the non-NCS portion of the CMT neuropathy score protocol, as previously described.[22] The score is referred to the clinical CMT neuropathy score ($CMTNS_C$) and is composed of scored evaluations (range 0–4) of sensory and motor symptoms in limbs, pin and vibration sensitivity, and limb muscle strength ($CMTNS_C$ range 0–28; higher scores indicate increased impairment). The portion of the $CMTNS_C$ taken from the legs ($CMTNS_L$ range 0–20) was also extracted for comparison to the MRI measures obtained in the legs.

Motor NCS data were acquired from the median or ulnar nerve of a majority of patients using conventional methods.[23] These data were acquired in the arms because NCS are often nonresponsive in the legs of patients with CMT.[24,25] Recording electrodes were placed over the bellies of hand thenar and hypothenar muscles, reference electrodes were placed over the tendons at the wrist, and stimulation was performed at the wrist distally and elbow proximally. The mean motor conduction velocity (MCV) and compound motor action potential (CMAP) are reported in the table.

Standard protocol approvals, registrations, and patient consents. Our local institutional review board approved this study, and signed consent was obtained prior to all examinations.

Table Summary MRI and clinical data

	Controls (n = 21)	CMT1A (n = 10)	CMT2A (n = 3)	HNPP (n = 3)
Age, y	40.0 ± 11.8 (23.4–58.1)	43.5 ± 10.7 (27.9–60.6)	39.9 ± 15.9 (25.8–57.1)	54.1 ± 11.6 (41.7–64.8)
BMI, kg/m^2	25.3 ± 5.4 (16.8–39.3)	24.3 ± 4.0 (18.6–30.7)	27.3 ± 2.4 (25.7–30.0)	29.1 ± 8.8 (22.5–39.1)
Male sex, %	47.6	40.0	66.7	66.7
MTR_v, pu	37.2 ± 2.3 (32.7–42.3)	33.8 ± 3.3 (27.8–37.3)	31.5 ± 1.9 (29.6–33.5)	34.4 ± 2.0 (32.3–36.1)
CSA_{SN}, mm^2	20.8 ± 4.8 (12.6–31.2)	41.9 ± 10.0 (22.8–55.1)	20.0 ± 4.8 (14.7–24.1)	26.0 ± 5.7 (20.8–32.1)
D_{SN}, mm	5.1 ± 0.6 (4.0–6.3)	7.2 ± 0.9 (5.4–8.3)	5.0 ± 0.7 (4.2–5.5)	5.7 ± 0.7 (5.0–6.4)
MCV,[a] m/s	—	25.2 ± 4.2 (20.0–32.0)[c]	53.8 ± 4.3 (50.0–58.5)	37.7 ± 3.5 (34.1–41.0)
CMAP,[a] mV	—	5.2 ± 2.8 (0.1–8.6)[c]	8.8 ± 1.8 (7.5–10.1)[e]	6.9 ± 2.5 (4.0–8.7)
$CMTNS_C$	0.0[b]	8.8 ± 5.4 (1.0–17.0)[d]	11.7 ± 3.5 (8.0–15.0)	10.3 ± 6.8 (5.0–18.0)
$CMTNS_L$	0.0[b]	6.9 ± 4.3 (1.0–14.0)[d]	10.3 ± 3.1 (7.0–13.0)	8.3 ± 4.2 (5.0–13.0)

Abbreviations: BMI = body mass index; CMAP = compound motor action potential; CMT1A = Charcot-Marie-Tooth type 1A; CMT2A = Charcot-Marie-Tooth type 2A; $CMTNS_C$ = clinical Charcot-Marie-Tooth neuropathy score; $CMTNS_L$ = leg-specific Charcot-Marie-Tooth neuropathy score; CSA_{SN} = cross-sectional area of the sciatic nerve; D_{SN} = diameter of the sciatic nerve; HNPP = hereditary neuropathy with liability to pressure palsies; MCV = motor conduction velocity; MTR_v = magnetization transfer ratio values calculated across the entire volume; pu = percent units.
Data collected in all subjects within each cohort unless otherwise stated and presented as mean ± SD (range).
[a] From median or ulnar nerve (or mean value when data from both nerves available).
[b] Collected in 1 control subject.
[c] Collected in a subset of 9 patients with CMT1A.
[d] Collected in a subset of 8 patients with CMT1A.
[e] Collected in a subset of 2 patients with CMT2A.

MTR data acquisition. MRI was performed using a 3.0T Philips Achieva MRI scanner (Philips Healthcare, Best, the Netherlands) and a 16-channel torso receive coil. MRI data were collected from a transverse volume in one thigh (figure 1). To measure MTR, multishot echoplanar imaging volumes were acquired with (magnetization transfer [MT]–weighted) and without (reference) application of an MT saturation pulse.[26] The MT pulse parameters were 25-ms single-lobe sinc pulse with Gaussian apodization, 1000° nominal flip angle, and 1.5 kHz off-resonance. Additional parameters included acquired/reconstructed resolution = 0.8 × 0.8 × 6 mm^3/0.75 × 0.75 × 3 mm^3, field of view = 192 × 192 × 144 mm^3, repetition time/echo time/excitation flip angle = 60 ms/11 ms/10°, *k*-space lines per shot = 5, SENSE factor = 1, signal acquisitions averaged = 2, and scan time ≈6 minutes. To minimize bias from fat near the nerve, a water-selective excitation pulse was employed. Previous work[27] demonstrated that large transmit radiofrequency, or B_1, variations in thigh skeletal muscle bias MTR values in an approximately linear fashion; therefore, we measured B_1 in the same volume as the MTR data using the actual flip-angle imaging approach.[28]

MTR data analysis. Data analyses were performed in MATLAB (Mathworks, Natick, MA) unless otherwise noted. When motion was detected, MIPAV's (NIH, Bethesda, MD) nonrigid registration tools were applied.[29] Following registration, MTR was calculated as follows:

$$MTR = (1 - S_{MT}/S_{REF}) \times 100 \text{ pu},$$

where S_{MT} and S_{REF} are the signal intensities in the MT-weighted and reference volumes, respectively—we use percent units (pu) instead of % to minimize ambiguity when talking about relative changes. B_1 was estimated[28] and the MTR values were corrected for B_1 variations as previously described.[27] Artifacts corrupted the B_1 correction scheme in 2 subjects. In these subjects, the change in MTR postcorrection was set to the overall median value to minimize bias from these artifacts.

Regions of interest (ROIs) were manually selected for the SN in the 40 central slices of the reference volume. These ROIs were then multiplied by mask generated using MIPAV's segmentation algorithm (fuzzy C-means), which eliminated background voxels as well as voxels that had been partially volume averaged with fat. Mean MTR values were calculated for each slice (MTR_s) and across the entire volume (MTR_v). The mean cross-sectional area of the SN (CSA_{SN}) was also estimated by multiplying the number of voxels in the ROI by the voxel's cross-sectional area. This was converted to an approximate diameter using the following:

$$D_{SN} = 2\sqrt{CSA_{SN}/\pi},$$

where D_{SN} is the diameter of the SN.

Repeatability studies. To assess interscan reliability, 6 control subjects underwent a second MRI at least 4 weeks after the first session. Inter-rater reliability was estimated in a subset of subjects (6 controls, 4 CMT1A, and 3 CTM2A) by having 2 raters (R.D.D. and L.M.D.) define ROIs as described above.

Statistics. Statistical analyses were performed using STATA/IC 13.1 (StataCorp, College Station, TX).

Tests were performed to evaluate (1) the relationship between MTR and confounding variables, (2) the variation of MTR across cohorts, (3) the relationship between MTR and disability, and (4) the repeatability of MTR. Significance was defined at the $\alpha = 0.05$ level for all tests.

We first examined the potential confounding influence of BMI, age, and sex on MTR_v via multiple linear regression in controls—a Shapiro–Wilk test on the regression residuals suggested normality ($p = 0.81$); therefore, parametric statistical tests were used throughout. The effects of BMI, age, and sex on MTR_v were quantified via Pearson partial correlation coefficients and were not significant in controls.

Assuming these results are translatable to the patient cohorts, we did not control for these factors in patients and a single-factor analysis of variance was employed to test for variation in MTR_v across cohorts. To test for significant differences between cohort pairs, post hoc analysis was performed using a Bonferroni multiple comparison test. Finally, correlations between MTR_v and

Figure 1 Representative anatomical images from each cohort

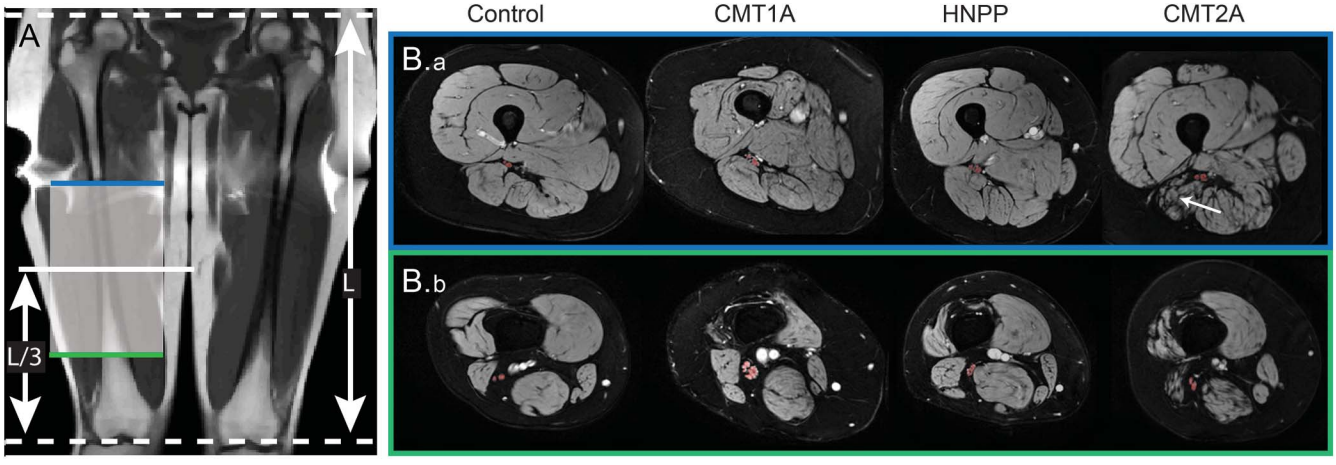

Representative coronal T_1-weighted scout image (A) and axial magnetization transfer (MT) images for each cohort (B). The length (L) of the femur was measured from the coronal scout image, and the axial MT volumes were centered 1/3 this length (L/3), as measured from the lower extremity. The most proximal (blue line, B.a) and distal slices (green line, B.b) are shown along with the region of interest (red overlay) for the sciatic nerve (SN). The tibial and common peroneal branches of the SN were resolvable in the more distal slices. Note the hypertrophy of the SN in the patient with Charcot-Marie-Tooth type 1A (CMT1A) and the muscle atrophy and fat replacement in the patient with Charcot-Marie-Tooth type 2A (CMT2A) (white arrow). HNPP = hereditary neuropathy with liability to pressure palsies.

disability scores were evaluated using linear regression analyses (with and without inclusion of the patients with unknown genetic causes) and Pearson correlation coefficients reported.

To understand the ability of MTR to provide estimates of treatment efficacy or disease evolution, it is important to understand the reliability of the acquisition (interscan) and assessment (inter-rater) methodology. To estimate the interscan reliability, intraclass correlation coefficients (ICC) were calculated for MTR_s and MTR_v. To test for changes in MTR_s and MTR_v across time, paired *t* tests were performed between each timepoint. Finally, the interscan variabilities of MTR_s and MTR_v were estimated via the repeatability coefficient (RC), which is defined as 1.96 times the SD of the mean difference in MTR between scans. Analogous analyses were performed for the inter-rater data.

RESULTS

Clinical features of patients. All patients with CMT had a typical history of chronic sensory loss, distal muscle weakness/atrophy, and foot deformities. Results from NCS (table) demonstrated uniform slowing of conduction velocities in patients with CMT1A (25.2 ± 4.2 m/s), while the conduction velocities were normal or minimally reduced in patients with CMT2A (53.8 ± 4.3 m/s). Three patients with HNPP, which is caused by a heterozygous deletion of the *PMP22* gene that is duplicated in CMT1A,[30] were also studied. Patients with HNPP reported transient, asymmetric, focal sensory loss and weakness following mechanical stresses; conduction velocities (37.7 ± 3.5 m/s) were between the values observed in CMT1A and control cohorts. Finally, patients with CMT with unknown genetic causes demonstrated the aforementioned symptoms and family history consistent with CMT as well as slowed conduction velocities (34.8 ± 8.1 m/s). Together, these results suggest that the patients studied represent typical populations of each disease.

General features of sciatic nerve MRI. Figure 1 shows sample coronal T_1-weighted scout images (left), axial MT data from each cohort (right), and user-defined ROIs (red overlay). The most proximal (blue line) and distal slices (green line) from the MT volume are shown. The SN was readily distinguished from surrounding fat (appears dark due to water-selective excitation pulse), muscle, and blood vessels in the proximal slices. Moving distally, the branching of the SN into the tibial and common peroneal nerves is evident. When defining the ROIs, both branches were labeled as SN. Consistent with previous work,[31] nerve hypertrophy was observed in the SN of patients with CMT1A (D_{SN} = 7.2 ± 0.9 mm, table). In contrast, mean nerve sizes in patients with CMT2A (D_{SN} = 5.0 ± 0.7 mm) and HNPP (D_{SN} = 5.7 ± 0.7 mm) were similar to values in controls (D_{SN} = 5.1 ± 0.6 mm). Finally, consistent with muscle pathology following denervation, varying degrees of muscle atrophy and fat infiltration were observed in patients (white arrow, figure 1).

MTR values are reduced in patients with CMT. Representative MTR maps from a control subject and patient with CMT1A (before and after B_1 correction) are shown in figure 2. Lower MTR values were observed in the SN of the patient with CMT1A (blue hues) relative to the control subject (yellow hues). The shading in MTR prior to correction scaled in an approximately linear fashion with the B_1 values, and most of this shading was removed with the correction strategy. In addition, the B_1 correction scheme improved the interscan repeatability of MTR_v (9% increase in ICC, 46% decrease in RC).

Scatterplots of MTR_v vs age and BMI are given in figure 3 (top row). In the control cohort, the effects of BMI (r^2 = 0.02, p = 0.56), age (r^2 = 0.03, p = 0.50), and sex (r^2 = 0.05, p = 0.34) on MTR_v were not significant. Results from the single-factor analysis of variance suggested that mean MTR_v values varied across cohorts ($p < 0.01$), and post hoc analysis detected differences between (1) control (37.2 ± 2.3 pu) and CMT1A (33.8 ± 3.3 pu; p = 0.01) and (2) control and CMT2A (31.5 ± 1.9 pu; $p < 0.01$) cohorts. MTR_v values were slightly reduced in patients with HNPP (34.4 ± 2.0 pu), but more data are needed to test whether this is significant.

MTR values correlate with neurologic disability in patients with CMT. Across subjects with a genetically confirmed diagnosis, a significant relationship was observed between MTR_v and $CMTNS_C$ (figure 3D: r^2 = 0.41, p = 0.01). For the leg-specific score ($CMTNS_L$), a stronger relationship was observed (r^2 = 0.49, $p < 0.01$). Within the CMT1A cohort, a trend toward significance was observed between MTR_v and $CMTNS_C$ (r^2 = 0.39, p = 0.10) and a significant relationship was observed for $CMTNS_L$ (r^2 = 0.51, p = 0.05). In contrast, no relationship was detected between nerve size and neuropathy scores (r^2 = 0.05, p = 0.43 for D_{SN} and $CMTNS_L$) or between NCS data and neuropathy scores (r^2 = 0.06/<0.01, p = 0.39/0.75 for MCV/CMAP and $CMTNS_L$). Finally, inclusion of the patients with CMT with unknown genetic cause did not significantly alter these correlations (r^2 = 0.22/0.33, p = 0.04/0.01 for MTR and $CMTNS_C$/$CMTNS_L$).

MTR values are repeatable. Sample interscan and inter-rater plots of MTR_s are shown in figure 4. As expected, MTR_v (ICC = 0.92, RC = 1.3 pu) showed a higher level of repeatability and lower level of variability than MTR_s (ICC = 0.69, RC = 3.1 pu) for the interscan data. In both cases, we did not detect a significant difference in MTR across time (p = 0.29 for MTR_s, p = 0.70 for MTR_v). For the inter-rater data, MTR_s (ICC = 0.99, RC = 0.8) and MTR_v (ICC > 0.99, RC = 0.2) values were nearly identical across raters.

Figure 2 Representative magnetization transfer ratio maps before and after B_1 correction

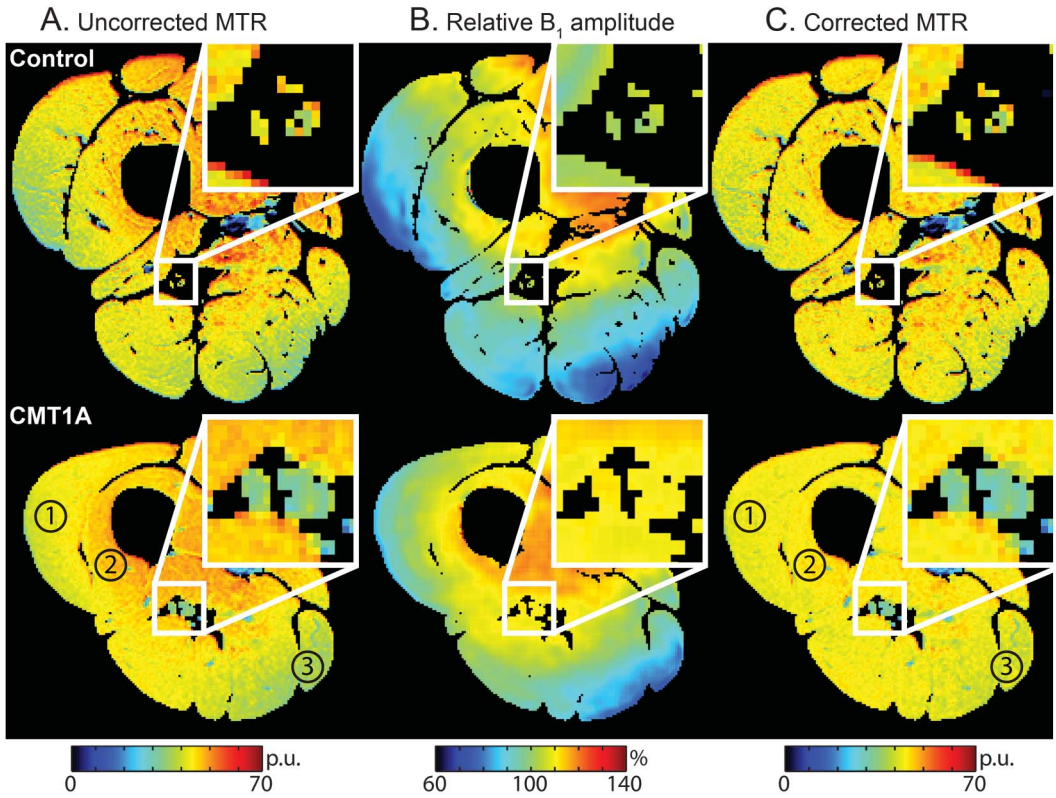

Representative uncorrected magnetization transfer ratio (MTR) maps (A), relative B_1 maps (B, B_1 given as a percentage of the desired value), and B_1-corrected MTR maps (C) from a control subject (top row) and patient with Charcot-Marie-Tooth type 1A (CMT1A) (bottom row). Slices were taken from center of the volume (at L/3 from the lower extremity as indicated in figure 1), and all images were masked to eliminate background voxels as well as voxels that had been partially volume averaged with fat. Note that most of the shading in the uncorrected MTR maps was removed by the B_1 correction process (the regions labeled 1, 2, and 3 in the uncorrected CMT1A map contain hues ranging from green to red, while the same regions in the corrected map contain more homogenous yellow hues). Consistent with the general trend (table), lower MTR values were observed in the sciatic nerve (zoomed inset) of the patient with CMT1A (blue hues) than the control subject (yellow hues).

DISCUSSION This study demonstrates that (1) proximal nerve pathology can be reliably assessed by MTR and (2) the resulting MTR values correlate with disability. This latter finding supports the potential use of proximal nerve MTR measurements as a biomarker in patients with CMT; the former supports the use of these measurements in future longitudinal studies (the lower limit detection for MTR_v changes is $\approx$1.5 pu). Interestingly, it appears that a relationship between proximal nerve MTR values and disability exists when looking across inherited neuropathy cohorts, including pathologically distinct cohorts such as HNPP, as well as when looking within the CMT1A cohort. In addition, the relationship between MTR and disability was strongest when confining our assessment to the legs ($CMTNS_L$). This suggests that MTR values in the SN specifically report on leg functions, which would be expected given that the SN is the primary conduit for motor and sensory information in the leg. In contrast, SN diameters (from MRI) and NCS-derived measures in median or ulnar nerves did not relate to disability.

One concern when examining novel MRI techniques is the confounding influence of comorbidities and demographic dispersion. Our results suggest that proximal nerve MTR values are largely independent of age, sex, and BMI. While previous work in white matter[32] has shown that MTR values vary with age, this relationship was found to be nonlinear, with values that are approximately constant over the age range studied. Interestingly, a similar relationship has been observed for diffusion metrics in nerve.[33] For MTR values of proximal nerve, additional data are needed to demonstrate whether such a relationship exists. Nevertheless, the effect of age (and BMI) on MTR was small in the current study; therefore, the observed differences are likely driven by pathologic rather than demographic factors.

Almost all conventional tests for human neuropathies target distal nerves. However, distal nerves are severely damaged in patients with CMT, producing a difficult-to-interpret floor effect when these tests are used as outcome measurements. For instance, NCS recordings on distal nerves are typically nonresponsive

Figure 3 Mean volumetric magnetization transfer ratio data for control subjects and patients with neuropathy

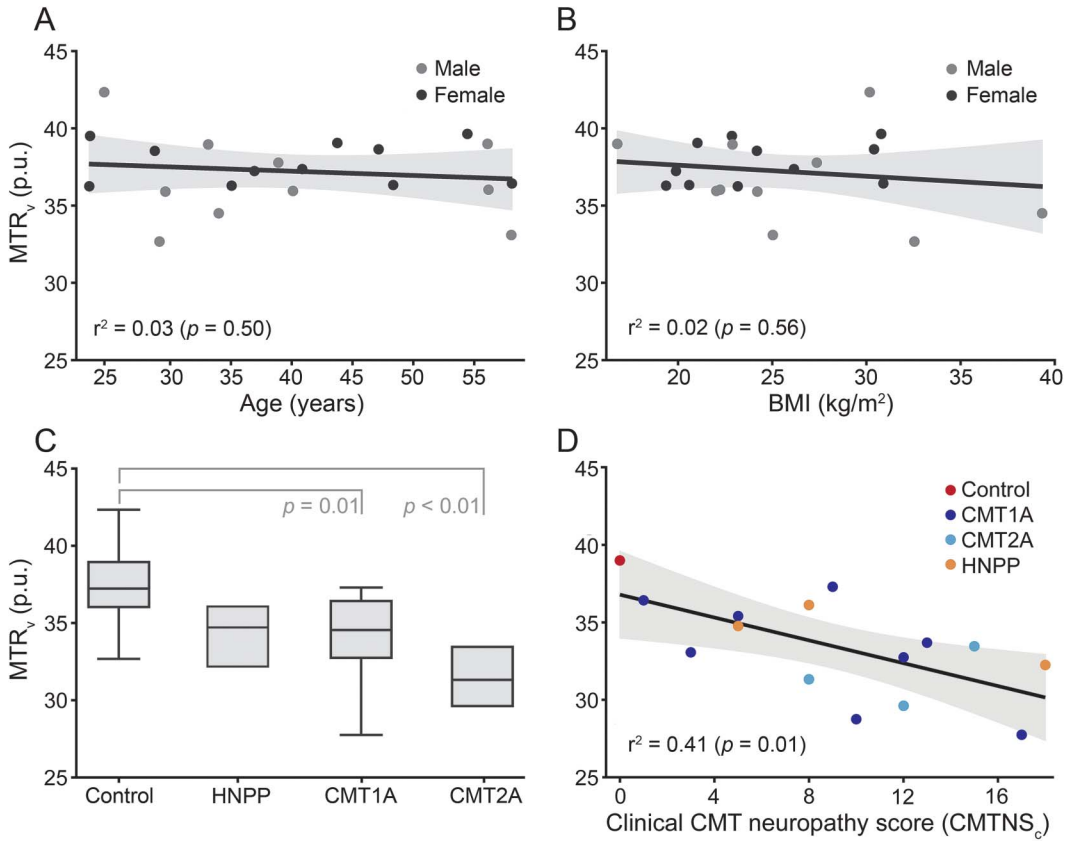

Scatterplots of magnetization transfer ratio values calculated across the entire volume (MTR_v) vs age (A) and body mass index (BMI) (B) are given for male (gray dots) and female (black dots) participants. Age, BMI, and sex did not have a significant effect on MTR_v in the control cohort. The boxplot of cohort MTR_v values (C) demonstrates the significant intercohort variation in MTR_v. Post hoc analysis identified significance between the following cohort pairs: control/Charcot-Marie-Tooth type 1A (CMT1A) and control/Charcot-Marie-Tooth type 2A (CMT2A). The scatterplot of MTR_v vs clinical Charcot-Marie-Tooth neuropathy score ($CMTNS_C$) (D) demonstrates the significant relationship between MTR_v and clinical disability. This regression was performed across control (red dots), CMT1A (dark blue), CMT2A (light blue), and hereditary neuropathy with liability to pressure palsies (HNPP) (orange) cohorts. In A, B, and D, the black lines are the result of a simple linear regression across all data in each scatterplot, and the shaded areas are the corresponding 95% confidence intervals.

in the lower limbs of patients with CMT.[24,25] In the upper limbs, sensory nerves are also typically nonresponsive, and even motor nerves can be nonresponsive in severe cases.[25,34] This longstanding obstacle, which limits the ability to longitudinally study CMT, may be overcome using proximal nerve MTR measurements. In addition, MTR measurements of proximal nerves may allow for insights into the neurobiology of CMT in humans—information previously available only via autopsy studies.[35] Axon–Schwann cell interactions play an important role in neurologic function[36]; therefore, anything that disrupts these interactions (e.g., demyelination, axonal loss) leads to nerve dysfunction. Previous work in white matter has shown that myelin lipids are the dominant source of MT,[37] and additional studies in peripheral nerve[20] have demonstrated that MTR correlates with myelin density. Given that myelin density is affected by demyelination/dysmyelination and axonal loss, MTR likely reports on the combined effect of these processes and, therefore, reports on disability. In addition, other factors that affect macromolecular content, such as changes in collagen content, may also modulate the observed MTR values in the peripheral nervous system.

Although promising, several limitations of this study should be addressed. First, a cross-sectional design was chosen to assess the effect of disease type, disability, and confounding variables (age, sex, and BMI) on nerve MTR values. This did not allow us to assess the sensitivity of the nerve MTR values to pathologic changes over time. Given that (1) diffusion MRI metrics of nerve have been shown to be sensitive to disease progression in other neuropathies[19] and (2) MTR and diffusion MRI probe complementary aspects of nerve pathology,[38] future longitudinal studies are needed. Second, a small number of patients were studied. Despite this limitation, a significant relationship was observed

Figure 4 Representative interscan and inter-rater data

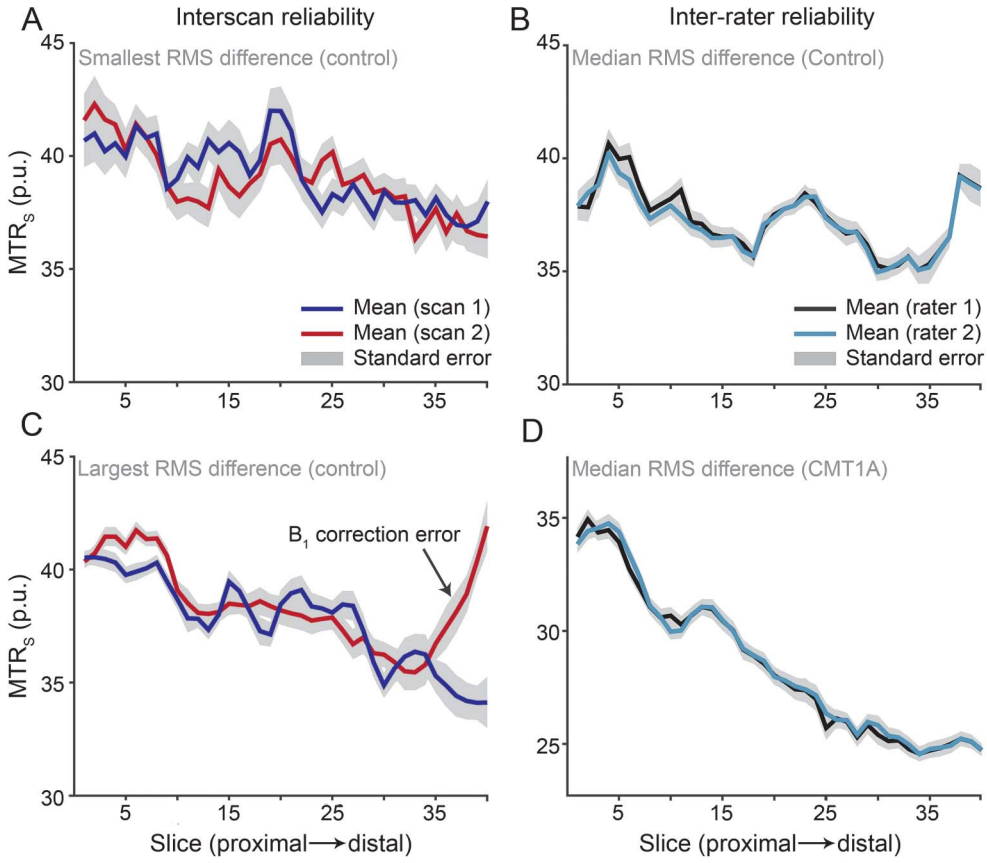

Representative interscan and inter-rater magnetization transfer ratio values calculated for each slice (MTR_S). For the interscan data, the control subjects with the smallest (A) and largest (C) root mean squared (RMS) difference across scans are given. The mean values across scans (red and dark blue lines) were repeatable at the slicewise (MTR_S) and volumetric levels (magnetization transfer ratio values calculated across the entire volume [MTR_V]); however, differences were observed in distal slices in a few subjects (see the MTR overcorrection in C, which is most likely due to artifacts in this subject's B_1 map). For the inter-rater data, the control (B) and patient (D) with the median RMS difference are given. In all cases, the mean values across raters (black and light blue lines) were highly repeatable.

between MTR and disability in patients with genetically confirmed CMT, and inclusion of patients with CMT without genetic confirmation did not alter this relationship. Thus, it appears that the results may be indicative of the larger population of patients with inherited neuropathies. Finally, MTR is a semiquantitative measure that is also sensitive to hardware settings/experimental parameters[39] as well as T_1 relaxation times.[40] The issue of hardware settings was mitigated via a B_1 correction scheme. Furthermore, from inspection of T_1-weighted images, it appears that T_1 values were not significantly altered in any subjects. For future multisite or longitudinal studies, however, protocol standardization or additional correction schemes[39] may be needed. In addition, quantitative MT approaches[40] should be explored, as these techniques yield parameters that are insensitive to the aforementioned issues that can affect MTR.

This study demonstrates that MTR measurements of the SN correlate with clinical disability in patients with CMT. The developed imaging protocols and data analysis pipelines resulted in highly repeatable MTR measurements. These results suggest that MTR measurements of proximal nerves may be of value as a biomarker, especially given that distal nerves are often fully degenerated in patients with CMT and proximal nerves are inaccessible via conventional techniques.

AUTHOR CONTRIBUTIONS

R.D.D.: drafting/revising the manuscript, study concept and design, analysis and interpretation of data, acquisition of data, statistical analysis, and funding support. L.M.D.: drafting/revising the manuscript, acquisition of data, and subject recruitment. J.C.G.: drafting/revising the manuscript, study concept, interpretation of data, and study supervision. S.A.S.: drafting/revising the manuscript, study concept, interpretation of data, statistical analysis, and funding support. J.L.: drafting/revising the manuscript, study concept and design, interpretation of data, acquisition of data, funding support, and study supervision.

ACKNOWLEDGMENT

The authors thank Ryan Alexander and Audra Hamilton for assistance with patient recruitment and logistics and MRI technologists Dave Pennell, Leslie McIntosh, Kristen George-Durrett, and Donna Butler for expertise and support.

STUDY FUNDING

Supported by NIH grants K25 EB013659 (R.D.D.), K01 EB009120 (S. A.S.), R01 NS066927 (J.L.), R21 NS081364 (J.L.), and U54 NS065712 (J.L.), as well as the National Center for Advancing Translational Sciences (CTSA award UL1TR000445; J.L.).

DISCLOSURE

The authors report no disclosures relevant to the manuscript. Go to Neurology.org for full disclosures.

Received April 1, 2014. Accepted in final form July 26, 2014.

REFERENCES

1. Dyck PJ, Lambert EH. Lower motor and primary sensory neuron diseases with peroneal muscular atrophy: I: neurologic, genetic, and electrophysiologic findings in hereditary polyneuropathies. Arch Neurol 1968;18:603–618.
2. Dyck PJ. Lower motor and primary sensory neuron diseases with peroneal muscular atrophy: II: neurologic, genetic, and electrophysiologic findings in various neuronal degenerations. Arch Neurol 1968;18:619–625.
3. Nelis E, Van Broeckhoven C, De Jonghe P, et al. Estimation of the mutation frequencies in Charcot-Marie-Tooth disease type 1 and hereditary neuropathy with liability to pressure palsies: a European collaborative study. Eur J Hum Genet 1996;4:25–33.
4. Dubourg O, Tardieu S, Birouk N, et al. The frequency of 17p11.2 duplication and Connexin 32 mutations in 282 Charcot-Marie-Tooth families in relation to the mode of inheritance and motor nerve conduction velocity. Neuromuscul Disord 2001;11:458–463.
5. Lupski JR, de Oca-Luna RM, Slaugenhaupt S, et al. DNA duplication associated with Charcot-Marie-Tooth disease type 1A. Cell 1991;66:219–232.
6. Raeymaekers P, Timmerman V, Nelis E, et al. Duplication in chromosome 17p11.2 in Charcot-Marie-Tooth neuropathy type 1A (CMT1A): the HMSN Collaborative Research Group. Neuromuscul Disord 1991;1:93–97.
7. Robertson AM, Perea J, McGuigan P, et al. Comparison of a new PMP22 transgenic mouse line with other mouse models and human patients with CMT1A. J Anat 2002; 200:377–390.
8. Verhoeven K, Claeys KG, Zuchner S, et al. MFN2 mutation distribution and genotype/phenotype correlation in Charcot-Marie-Tooth type 2. Brain 2006;129:2093–2102.
9. Zuchner S, Mersiyanova IV, Muglia M, et al. Mutations in the mitochondrial GTPase Mitofusin 2 cause Charcot-Marie-Tooth neuropathy type 2A. Nat Genet 2004;36: 449–451.
10. Shy ME, Blake J, Krajewski K, et al. Reliability and validity of the CMT neuropathy score as a measure of disability. Neurology 2005;64:1209–1214.
11. Ebenezer GJ, Hauer P, Gibbons C, McArthur JC, Polydefkis M. Assessment of epidermal nerve fibers: a new diagnostic and predictive tool for peripheral neuropathies. J Neuropathol Exp Neurol 2007;66:1059–1073.
12. Pareyson D, Reilly MM, Schenone A, et al. Ascorbic acid in Charcot-Marie-Tooth disease type 1A (CMT-TRIAAL and CMT-TRAUK): a double-blind randomised trial. Lancet Neurol 2011;10:320–328.
13. Lewis RA, McDermott MP, Herrmann DN, et al. High-dosage ascorbic acid treatment in Charcot-Marie-Tooth disease type 1A: results of a randomized, double-masked, controlled trial. JAMA Neurol 2013;70:981–987.
14. Padua L, Pareyson D, Aprile I, et al. Natural history of Charcot-Marie-Tooth 2: two-year follow-up of muscle strength, walking ability and quality of life. Neurol Sci 2010;31:175–178.
15. Chung KW, Suh BC, Shy ME, et al. Different clinical and magnetic resonance imaging features between Charcot-Marie-Tooth disease type 1A and 2A. Neuromuscul Disord 2008;18:610–618.
16. Sinclair CD, Morrow JM, Fischmann A, et al. Novel muscle fat-fraction MRI metrics for quantifying neuromuscular pathology. Neuromuscul Disord 2012;22:S33.
17. Sinclair CDJ, Morrow JM, Miranda MA, et al. Skeletal muscle MRI magnetisation transfer ratio reflects clinical severity in peripheral neuropathies. J Neurol Neurosurg Psychiatry 2012;83:29–32.
18. Kakuda T, Fukuda H, Tanitame K, et al. Diffusion tensor imaging of peripheral nerve in patients with chronic inflammatory demyelinating polyradiculoneuropathy: a feasibility study. Neuroradiology 2011;53:955–960.
19. Mathys C, Aissa J, Meyer Zu Hörste G, et al. Peripheral neuropathy: assessment of proximal nerve integrity by diffusion tensor imaging. Muscle Nerve 2013;48:889–896.
20. Odrobina E, Lam T, Pun T, Midha R, Stanisz GJ. MR properties of excised neural tissue following experimentally induced demyelination. NMR Biomed 2005;18:277–284.
21. Gambarota G, Veltien A, Klomp D, Van Alfen N, Mulkern RV, Heerschap A. Magnetic resonance imaging and T_2 relaxometry of human median nerve at 7 Tesla. Muscle Nerve 2007;36:368–373.
22. Murphy SM, Herrmann DN, McDermott MP, et al. Reliability of the CMT neuropathy score (second version) in Charcot-Marie-Tooth disease. J Peripher Nerv Syst 2011; 16:191–198.
23. Li J, Krajewski K, Shy ME, Lewis RA. Hereditary neuropathy with liability to pressure palsy: the electrophysiology fits the name. Neurology 2002;58:1769–1773.
24. Lewis RA, Sumner AJ, Shy ME. Electrophysiological features of inherited demyelinating neuropathies: a reappraisal in the era of molecular diagnosis. Muscle Nerve 2000;23:1472–1487.
25. Li J. Inherited neuropathies. Semin Neurol 2012;32:204–214.
26. Smith SA, Farrell JAD, Jones CK, Reich DS, Calabresi PA, van Zijl PC. Pulsed magnetization transfer imaging with body coil transmission at 3 Tesla: feasibility and application. Magn Reson Med 2006;56:866–875.
27. Sinclair CD, Morrow JM, Hanna MG, et al. Correcting radiofrequency inhomogeneity effects in skeletal muscle magnetisation transfer maps. NMR Biomed 2012;25: 262–270.
28. Yarnykh VL. Actual flip-angle imaging in the pulsed steady state: a method for rapid three-dimensional mapping of the transmitted radiofrequency field. Magn Reson Med 2007;57:192–200.
29. Vercauteren T, Pennec X, Perchant A, Ayache N. Diffeomorphic demons: efficient non-parametric image registration. Neuroimage 2009;45(1 suppl):S61–S72.
30. Li J, Parker B, Martyn C, Natarajan C, Guo J. The *PMP22* gene and its related diseases. Mol Neurobiol 2013;47:673–698.
31. Sinclair CDJ, Morrow JM, Fischmann A, et al. MRI shows increased tibial nerve size in CMT1A. Neuromuscul Disord 2011;21:S28.

32. Ge Y, Grossman RI, Babb JS, Rabin ML, Mannon LJ, Kolson DL, et al. Age-related total gray matter and white matter changes in normal adult brain: part II: quantitative magnetization transfer ratio histogram analysis. ANJR Am J Neuroradiol 2002;23:1334–1341.
33. Tanitame K, Iwakado Y, Akiyama Y, et al. Effect of age on the fractional anisotropy (FA) value of peripheral nerves and clinical significance of the age-corrected FA value for evaluating polyneuropathies. Neuroradiology 2012;54: 815–821.
34. Krajewski KM, Lewis RA, Fuerst DR, et al. Neurological dysfunction and axonal degeneration in Charcot-Marie-Tooth disease type 1A. Brain 2000;123:1516–1527.
35. Li J, Bai Y, Ianakova E, et al. Major myelin protein gene (P0) mutation causes a novel form of axonal degeneration. J Comp Neurol 2006;498:252–265.
36. Li J. Hypothesis of double polarization. J Neurol Sci 2008; 275:33–36.
37. Koenig S. Cholesterol of myelin is the determinant of gray-white contrast in MRI of brain. Magn Reson Med 1991;20:285–291.
38. Underhill HR, Yuan C, Yarnykh VL. Direct quantitative comparison between cross-relaxation imaging and diffusion tensor imaging of the human brain at 3.0 T. Neuroimage 2009;47:1568–1578.
39. Berry I, Barker G, Barkhof F, et al. A multicenter measurement of magnetization transfer ratio in normal white matter. J Magn Reson Imaging 1999;9:441–446.
40. Henkelman RM, Huang X, Xiang QS, Stanisz GJ, Swanson SD, Bronskill MJ. Quantitative interpretation of magnetization transfer. Magn Reson Med 1993;29: 759–766.